JACC: CARDIOVASCULAR IMAGING VOL. 5, NO. 9, 2012

ISSN 1936-878X/$36.00
PUBLISHED BY ELSEVIER INC. http://dx.doi.org/10.1016/j.jcmg.2012.03.015

Acute Left Ventricular Remodeling Following Myocardial Infarction

Coupling of Regional Healing With Remote Extracellular Matrix Expansion

William Chan, MBBS, PhD,*† Stephen J. Duffy, MBBS, PhD,*† David A. White, BSc,† Xiao-Ming Gao, MBBS, MD,† Xiao-Jun Du, MBBS, PhD,† Andris H. Ellims, MBBS,*† Anthony M. Dart, BM, BCh, DPhil,*†‡ Andrew J. Taylor, MBBS, PhD*†

Melbourne, Australia

OBJECTIVES This prospective study aimed to assess regional and temporal patterns of extracellular matrix (ECM) changes post-myocardial infarction (MI).

BACKGROUND A fundamental process in the development of ischemic left ventricular (LV) dysfunction is LV remodeling, characterized by structural and functional abnormalities throughout the myocardium including the noninfarcted (remote) myocardium and interstitium.

METHODS Contrast-enhanced cardiac magnetic resonance (CMR) was performed on MI patients acutely (mean: 5 days post-MI, n = 25) and repeated subacutely (mean: 139 days post-MI, n = 21), and was also performed in a separate group of 15 patients with chronic MI (mean: 2,580 days post-MI, n = 15). Twenty volunteers without a history of MI acted as controls. CMR was used to evaluate LV morphology and function, with post-contrast T1 mapping to semiquantitatively assess changes in the ECM. Putative mediators of myocardial inflammation and fibrosis, including macrophage migration inhibitory factor (MIF), were also measured.

RESULTS Age, sex, and diabetic and hypertensive status did not differ between MI groups and controls. Compared with controls, patients early post-acute MI demonstrated reduced LV ejection fraction (50.25 ± 7.29% vs. 66.7 ± 6.2% [controls], $p < 0.0001$). Myocardium remote to the infarction early post-acute MI, compared with controls, demonstrated reduced systolic thickening (60 ± 5.0% vs. 106 ± 7.6%, $p \leq 0.0002$), and lower post-contrast myocardial T1 times suggestive of ECM expansion (437 ± 113 ms vs. 549 ± 119 ms, $p = 0.01$). In a subgroup analysis between early post-acute MI and controls of similar age and sex, the remote sector post-contrast myocardial T1 times remained significantly shorter post-acute MI compared with controls (420 ± 121 ms vs. 529 ± 113 ms, $p = 0.03$). Serum levels of MIF inversely correlated with global myocardial T1 time in patients early post-acute MI ($r = -0.6$, $p = 0.01$), suggesting a coupling of regional healing with acute LV remodeling.

CONCLUSIONS Within a week of acute MI, the remote myocardium exhibits systolic dysfunction and expansion of the ECM, which is coupled with physiological infarct healing. Further prospective studies with larger sample sizes are needed to verify these important findings. (J Am Coll Cardiol Img 2012;5:884–93) © 2012 by the American College of Cardiology Foundation

From the *Department of Cardiovascular Medicine, Alfred Hospital, Melbourne, Australia; †Baker IDI Heart and Diabetes Institute, Melbourne, Australia; and the ‡Department of Medicine, Monash University, Melbourne, Australia. Dr. Chan is supported by a postgraduate scholarship from the National Health and Medical Research Council of Australia and a support grant from GlaxoSmithKline Australia. Mr. White is supported by an Australian National Heart Foundation PhD Scholarship (PB 10M 5481). Drs. Duffy, Du, Dart, and Taylor are supported by a National Health and Medical Research Council Program Grant. Dr. Taylor is also supported by a National Heart Foundation Grant, Melbourne, Australia. Dr. Gao is supported by a National Health and Medical Research Council Project Grant. All other authors have reported that they have no relationships relevant to the contents of this paper to disclose.

Manuscript received November 8, 2011; revised manuscript received February 22, 2012, accepted March 9, 2012.

A fundamental process in the development of ischemic left ventricular (LV) dysfunction is LV remodeling, characterized by structural and functional abnormalities occurring throughout the myocardium (1). This paradigm of LV remodeling is based on the concept that structural changes in the infarct zone result in adverse LV wall stress in the noninfarct zone, and with time, progressive LV dilation and dysfunction ensue (2,3). Diffuse myocardial fibrosis, which represents an important histological hallmark of end-stage cardiomyopathy in humans (1,4), may develop in the noninfarcted myocardium early after acute myocardial infarction (MI) in animals (5–8). However, to what extent diffuse myocardial fibrosis contributes to LV remodeling remains uncertain (1,3). The extent of myocardial fibrosis development following MI has important prognostic implications because therapy with aldosterone receptor antagonists, which possess antifibrotic properties, improves clinical outcomes (9–11).

See page 894

Gadolinium-based contrast can accumulate throughout the myocardium when the extracellular matrix (ECM) is diffusely expanded due to increased collagen deposition, with prior animal studies showing a correlation between myocardial T1 relaxation time and total collagen content (12). Post-contrast myocardial T1 mapping has been validated to semiquantitatively detect diffuse myocardial fibrosis in patients with chronic heart failure (4), aortic stenosis, and hypertrophic cardiomyopathy (13). We hypothesized that there may be acute expansion of the ECM suggestive of a diffuse fibrotic response post-acute MI in the noninfarcted (remote) myocardium that may contribute to LV remodeling. We utilized contrast-enhanced cardiac magnetic resonance (CMR) to assess LV remodeling in patients post-MI and measured serum N-terminal propeptides of type I and III procollagen (PINP and PIIINP, respectively) to evaluate myocardial collagen turnover (9,11). Putative mediators of myocardial inflammation and fibrosis, including macrophage migration inhibitory factor (MIF) (14–16) and transforming growth factor-β1 (TGF-β1) (8,17), were sampled to explore any association of infarct healing with regional and global myocardial T1 times.

METHODS

CMR with post-contrast myocardial T1 mapping was performed in 2 groups of participants at varying time points post-MI (acute, subacute, and chronic) and in a group of controls without prior MI. All research was performed at the Alfred Hospital, Melbourne, Australia, between June 2009 and January 2011 following approval by the Alfred Hospital Human Research Ethics Committee. All patients provided informed written consent.

Study participants. EARLY POST-ACUTE MI GROUP. Consecutive patients >18 years old with first-presentation ST-segment elevation MI due to single-vessel coronary occlusion were invited to participate following percutaneous coronary intervention (PCI). Patients having 1 or more of the following criteria were excluded: an intracardiac device or metallic prosthesis not compatible with CMR (e.g., pacemaker); severe claustrophobia; and renal impairment (estimated glomerular filtration rate ≤60 ml/min).

SUBACUTE MI GROUP. All enrolled patients post-acute MI were invited to return for a follow-up CMR examination 3 to 6 months following their index admission, forming the subacute MI group.

CHRONIC MI GROUP. A separate group of patients with prior MI formed the chronic MI group. These patients either had a history of single-vessel coronary artery disease on coronary angiography in a setting of prior MI ≥6 months ago or a remote history of MI without current evidence of ischemia documented by nuclear perfusion imaging.

CONTROL GROUP. Volunteers with normal LV systolic function, no structural heart disease, and no symptoms of heart failure or MI formed the control group.

CMR protocol. CMR studies were performed on a clinical 1.5-T CMR scanner (Signa HDx 1.5T, GE Healthcare, Waukesha, Wisconsin). All analyses were performed offline using ReportCARD version 3.6 (for LV volumetric and infarct size assessment) and VizPack Application version 7.3.0 (GE Healthcare, Waukesha, Wisconsin) (for T1 mapping and regional LV function assessment).

ASSESSMENT OF LV VOLUME AND FUNCTION. In controls, a bright-blood 2-dimensional steady-state free precession pulse sequence was employed to obtain cine imaging in 3 apical standard echocardi-

ABBREVIATIONS AND ACRONYMS

CMR = cardiac magnetic resonance
ECM = extracellular matrix
LGE = late gadolinium enhancement
LV = left ventricle/ventricular
LVEF = left ventricular ejection fraction
MI = myocardial infarction
MIF = macrophage migration inhibitory factor
MS = myocardial sector
NT-proBNP = N-terminal pro–B-type natriuretic peptide
PCI = percutaneous coronary intervention
PIIINP = N-terminal propeptide of type III procollagen
PINP = N-terminal propeptide of type I procollagen
STIR = short-tau inversion recovery
TGF = transforming growth factor

ography views (4). In MI patients, LV systolic function and ejection fraction (LVEF) were calculated by volumetric analysis (18). Additionally, separate cine views were acquired in 3 short-axis slices (basal, midventricular, and apical) for comparison with T1 mapping and edema sequences as described in the following text. Regional wall thickness and systolic thickening assessments were performed from the basal, mid, and apical short-axis slices by calculating the end-diastolic and end-systolic wall thicknesses as well as the percentage systolic thickening (19).

MYOCARDIAL EDEMA ASSESSMENT. T2-weighted short-tau inversion recovery (STIR) fast spin echo images were acquired in 3 short-axis slices (basal, midventricular, and apical) to quantify myocardial edema (20). A relative STIR ratio of >2.2 was used to define the presence of myocardial edema (20).

MI SIZE QUANTIFICATION. Late gadolinium enhancement (LGE) imaging was performed 10 to 15 min after a bolus of gadolinium–diethylenetriamine pentaacetic acid (DTPA) (0.2 mmol/kg, Magnevist, Bayer Schering Pharma, Leverkusen, Germany) using an inversion recovery gradient echo technique on the LV short-axis stack as for volumetric analysis. The area of hyperenhanced myocardium (bounded by endocardial and epicardial contours) on each of the short-axis slices was manually traced, and then multiplied by the slice thickness and the myocardial density of 1.05 g/ml to obtain the infarct mass.

POST-CONTRAST MYOCARDIAL T1 MAPPING. T1 mapping was performed on a set of 10 images obtained by employing varying inversion times (75 to 750 ms) acquired 15 to 20 min after bolus gadolinium-DTPA using an inversion recovery–prepared fast gradient echo sequence at the basal, midventricular, and apical short-axis views (4). These images were then processed with a curve-fitting technique to generate T1 maps using a dedicated research software package (Fig. 1). Only T1 maps with an R-squared value for the curve fit of >0.95 were used in the analysis.

MYOCARDIAL SECTORING FOR EDEMA, INFARCT, T1 MAPPING, AND REGIONAL SYSTOLIC THICKENING ASSESSMENT. In all patients, we subdivided each of the 3 short-axis LGE slices into 6 equal circumferential sectors (with 60° arc) (Fig. 1) to generate 18 myocardial sectors (MS) per patient (21). We defined MS1 as the point of right ventricular insertion into the LV at end-diastole. A sector with

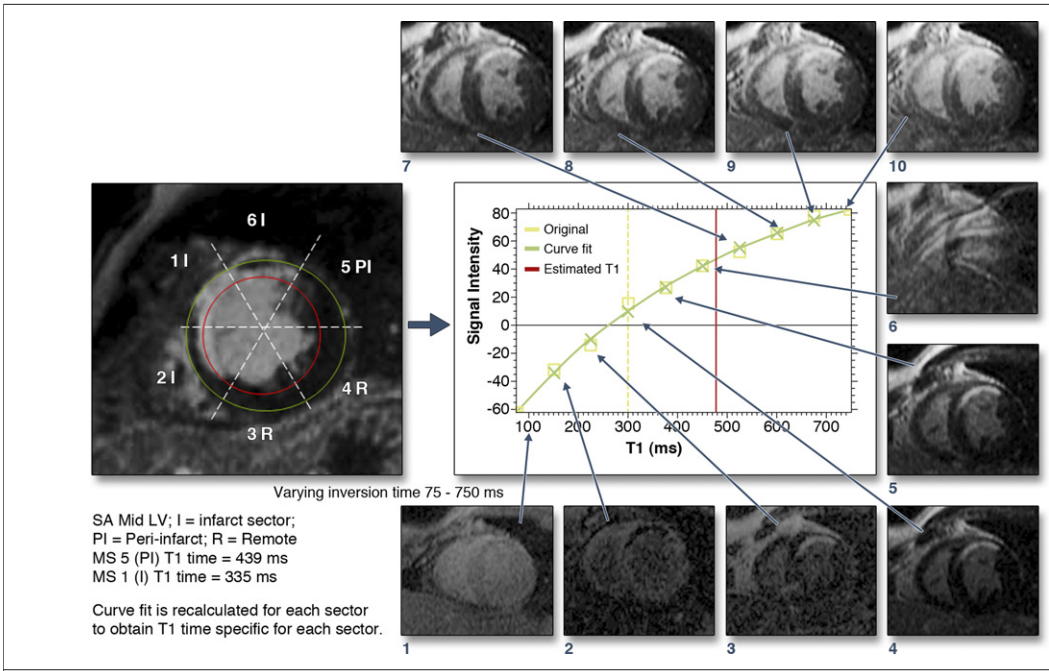

Figure 1. Myocardial Sectoring and T1 Mapping

Myocardial sectoring was performed by subdividing each of the 3 short-axis (mid-LV shown in this schema) LGE slices into 6 equal circumferential sectors (with 60° arc). Only T1 maps with an R-squared value for the curve fit of >0.95 were used in the analysis. A specific T1 time was calculated for each myocardial sector. LGE = late gadolinium enhancement; LV = left ventricle; MS = myocardial sector; SA = short-axis.

LGE visible in >50% of the arc of the sector (i.e., >30°) was defined as an infarct sector, whereas a peri-infarct sector was defined as having any LGE within the sector. A remote sector was defined as any sector with no LGE. Myocardial sectoring was then applied in the same fashion to cine, STIR, and T1 images. In some patients without anterior or anteroseptal infarction, MS1 and MS2 appeared bright because of flow artifact created by the LV outflow tract. These sectors were excluded from all analyses. Areas of extensive microvascular obstruction were also excluded from T1 mapping analysis.

Biochemical analysis. All routine biochemistries were analyzed by the Alfred Hospital Pathology Service. TGF-β1 was measured in sera in duplicates using enzyme-linked immunosorbent assay (Life Research, Scoresby, Victoria, Australia). MIF was measured in plasma in duplicates by enzyme-linked immunosorbent assay (DuoSet human MIF, cat# DY289, R&D Systems, Minneapolis, Minnesota) (14). PINP was determined by electrochemiluminescence immunoassay using a commercially available radioimmunoassay kit (Cobas, Roche Diagnostics, Basel, Switzerland). PIIINP measurements were performed using a commercially available radioimmunoassay kit (UniQ, Orion Diagnostica, Espoo, Finland). Serum N-terminal pro–B-type natriuretic peptide (NT-proBNP) concentration was determined using electrochemiluminescence immunoassay on the Roche E170 analyzer (Roche Diagnostics).

Statistical analysis. Continuous, normally distributed data were expressed as mean ± SD, and categorical variables were presented as counts and percentages. Sample size calculation was based on our prior study that demonstrated that controls had a myocardial T1 time of 564 ± 103 ms (4). Thus, based on an expected difference in T1 time of 20%, and using a standard deviation of 103 ms, we calculated that a sample size of 15 per group would be required to achieve a desired power of 0.80 with an alpha value of 0.05. Continuous variables were compared with either paired or unpaired Student *t* tests, or 1-way analysis of variance with Bonferroni correction. Categorical variables were compared between groups with a chi-square or Fisher exact test where appropriate. Correlation between continuous parameters was assessed with Pearson's product-moment correlation coefficient. A subgroup analysis between early post-acute MI and control participants of similar age and sex was performed to examine differences in myocardial T1 time in the remote myocardium. Values of $p < 0.05$ were considered statistically significant. All analyses were performed with SPSS version 16 (SPSS Inc., Chicago, Illinois).

Table 1. Baseline Characteristics

	Control (n = 20)	Early Post-Acute MI (n = 25)	Chronic MI (n = 15)	p Value
Age, yrs	54.7 ± 10.2	58.6 ± 8.8	59.4 ± 12.8	NS
Age of infarct, days	NA	4.8 ± 4.7	2,580.3 ± 2,472.5	
		3.5 [3–5.5]	2,366 [259–4,444]	
Male	13 (65%)	20 (88%)	12 (80%)	NS
Hypertension	8 (40%)	8 (32%)	7 (47%)	NS
Current smoking	0 (0%)	12 (48%)	4 (27%)	**0.001***†
Diabetes	0 (0%)	3 (12%)	2 (13%)	NS
Body mass index, kg/m^2	27.0 ± 4.2	26.7 ± 3.0	28.7 ± 2.9	NS
Anterior MI	NA	10 (40%)	10 (67%)	NS
Heart rate, beats/min	66 ± 16	69 ± 8	62 ± 8	NS
eGFR, ml/min	97.0 ± 39.5	95.1 ± 26.9	77.8 ± 21.3	NS
Medications				
Aspirin	0 (0%)	25 (100%)	14 (93%)	**<0.001***†
Angiotensin-converting enzyme inhibitors	6 (30%)	21 (84%)	12 (80%)	**<0.0001***†
Angiotensin-receptor blockers	1 (5%)	2 (8%)	1 (7%)	NS
Aldosterone-receptor antagonists	0 (0%)	4 (16%)	2 (13%)	NS
Beta-blocker	4 (20%)	22 (88%)	13 (87%)	**<0.0001***†
Statins	0 (0%)	23 (92%)	14 (93%)	**<0.0001***†
Primary PCI	NA	25 (100%)	8 (53%)	NS

Values are n (%) or mean ± SD, or median [interquartile range]. p values in **bold** are statistically significant. *Control versus early post-acute MI; †control versus chronic MI.
eGFR = estimated glomerular filtration rate; MI = myocardial infarction; PCI = percutaneous coronary intervention; NS = not significant.

RESULTS

Clinical and demographic data. A total of 60 patients were enrolled, with 25 patients in the early post-acute MI group, 15 patients in the chronic MI group, and 20 controls (Table 1). We performed repeat CMR and biomarker evaluation in 21 of 25 early post-acute MI patients, which formed the subacute MI group. Age, sex, body mass index, diabetic status, and hypertensive status were similar across all groups (p = NS). The mean infarct age was 4.8 ± 4.7 days, 139.2 ± 54.7 days, and 2,580.3 ± 2,472.5 days in the early post-acute, subacute, and chronic MI groups, respectively. All early post-acute (and subacute) MI patients underwent primary PCI, whereas only one-half of the chronic MI group were reperfused by primary PCI (100% vs. 53%, p = 0.09). Heart rate and renal function were not different across all 3 groups (Table 1).

LV volume, function, and infarct characteristics. Patients early post-acute MI had greater infarct mass and infarct size compared with the chronic MI group (Table 2). There was an increase between control, early post-acute MI, and chronic MI groups with respect to indexed LV end-systolic volume (all p < 0.01) and between control and chronic MI LV end-diastolic volume (p = 0.01). LVEF was lowest among patients early post-acute MI and highest in controls (50.2 ± 7.3% vs. 66.6 ± 6.2%, p < 0.0001). Compared with controls, both early post-acute and chronic MI groups demonstrated a reduction in regional systolic thickening in the remote sectors (acute: 59.6 ± 24.6%, chronic: 68.4 ± 32.6%, control: 105.6 ± 34.1%, p ≤ 0.002), consistent with remodeling of the remote (noninfarcted) myocardium (Table 2). CMR examination in subacute MI patients demonstrated persistence of changes identified acutely with respect to increased LV volumes (90.3 ± 26.0 ml/m^2 vs. 85.8 ± 16.5 ml/m^2, p = NS) and reduced regional systolic function in infarct (65.0 ± 36.5% vs. 57.5 ± 31.9%, p = NS), peri-infarct (70.8 ± 38.2% vs. 55.8 ± 23.0%, p = NS), and remote regions (67.0 ± 27.9% vs. 59.6 ± 24.6%, p = NS) (Table 3).

Post-contrast myocardial T1 times. Post-contrast myocardial T1 times were reduced in the infarct sectors compared with controls in both early post-acute and chronic MI groups (319 ± 64 ms vs. 549 ± 119 ms and 323 ± 65 ms vs. 549 ± 119 ms, respectively, all p < 0.0001) (Fig. 2). Peri-infarct sector post-contrast T1 times were significantly shorter in patients early post-acute MI compared with controls. Additionally, remote post-contrast T1 times in early post-acute MI patients were also significantly shorter than controls (437 ± 113 ms vs. 549 ± 119 ms, p = 0.01), suggestive of ECM expansion in these regions. There was a strong trend to shorter post-contrast T1 times in remote sectors of chronic MI patients compared with controls (464 ± 117 ms vs. 549 ± 119 ms, p =

Table 2. LV Volume, Function, and Infarct Characteristics by CMR

	Control	Early Post-Acute MI	Chronic MI	p Value
Body surface area, m^2	1.9 ± 0.3	2.0 ± 0.2	2.0 ± 0.2	NS
LV mass indexed, g/m^2	60.6 ± 15.4	74.0 ± 13.8	64.6 ± 13.8	**0.01***
Delayed enhancement, g	NA	28.6 ± 18.6	16.0 ± 7.6	**0.03‡**
Myocardial infarct size, %	NA	19.2 ± 10.5	12.73 ± 5.0	**0.05‡**
LVEF, %	66.6 ± 6.2	50.2 ± 7.3	51.2 ± 12.7	**<0.0001*†**
LVEDVi, ml/m^2	77.0 ± 16.9	85.8 ± 16.5	97.3 ± 24.6	**0.01†**
LVESVi, ml/m^2	26.7 ± 9.3	42.9 ± 12.7	50.1 ± 27.3	**<0.01*†**
Infarct ESWT, mm	NA	8.4 ± 1.5	8.1 ± 2.3	NS
Infarct EDWT, mm	NA	5.6 ± 1.2	5.3 ± 1.2	NS
Infarct ESWT, %	NA	57.5 ± 31.9	62.8 ± 46.2	NS
Peri-infarct ESWT, mm	NA	8.4 ± 1.4	9.3 ± 2.9	NS
Peri-infarct EDWT, mm	NA	5.6 ± 0.8	5.4 ± 1.3	NS
Peri-infarct ESWT, %	NA	55.8 ± 23.0	80.1 ± 37.5	**0.02‡**
Remote ESWT, mm	9.9 ± 2.0	8.8 ± 1.3	8.6 ± 2.6	NS
Remote EDWT, mm	5.2 ± 1.3	5.8 ± 1.1	5.2 ± 0.9	NS
Remote ESWT, %	105.6 ± 34.1	59.6 ± 24.6	68.4 ± 32.6	**≤0.002*†**

Values are mean ± SD. p values in **bold** are statistically significant. *Control versus early post-acute MI; †control versus chronic MI; ‡early post-acute versus chronic MI.

CMR = cardiac magnetic resonance; EDWT = end-diastolic wall thickness; ESWT = end-systolic wall thickness; ESWT% = percentage end-systolic wall thickening; LV = left ventricular; LVEDVi = left ventricular end-diastolic volume index; LVEF = left ventricular ejection fraction; LVESVi = left ventricular end-systolic volume index; NA = not applicable; other abbreviations as in Table 1.

0.07). Similarly, global myocardial T1 times were shorter in early post-acute and chronic MI patients compared with controls (all $p \leq 0.005$). Compared with early post-acute MI patients, post-contrast T1 times were increased in the subacute MI group in peri-infarct (395 ± 62 ms vs. 446 ± 74 ms, $p = 0.04$) and remote sectors (434 ± 93 ms vs. 515 ± 68 ms, $p = 0.01$) (Table 3).

To exclude age and sex as confounding variables for myocardial T1 time changes in remote regions, we performed a separate subgroup analysis in 15 early post-acute MI and 11 control participants of similar age and sex in which remote post-contrast myocardial T1 times remained significantly shorter post-acute MI compared with controls (420 ± 121 ms vs. 529 ± 11 3 ms, $p = 0.03$). There were no significant differences in the mean heart rate between control and MI groups before CMR examination (control: 66 ± 16 beats/min, early post-acute MI: 69 ± 8 beats/min, chronic: 62 ± 8 beats/min, all $p > 0.05$), excluding heart rate as a confounding factor in the measurement of myocardial T1 time (4). Furthermore, the remote myocardial T1 times in the early post-acute MI group were not different among patients who were diabetic versus nondiabetic patients, and smokers versus nonsmokers (p = NS for all comparisons).

Significant positive correlations were observed between early post-acute and subacute MI mean global T1 times with LVEF ($r = 0.4$, $p = 0.05$; and $r = 0.5$, $p = 0.03$, respectively). There was also a positive correlation between chronic MI global T1 time and LVEF ($r = 0.5$, $p = 0.06$).

A small number of MS could not be analyzed due to artifact, microvascular obstruction, or poor curve fit (early post-acute MI: 74 of 450 = 16%; subacute MI: 19 of 378 = 5%; chronic MI: 25 of 270 = 9%).

Myocardial edema. The mean infarct STIR ratio was elevated early post-acute MI compared with chronic MI (3.0 ± 0.4 vs. 1.9 ± 0.2, $p < 0.0001$) and subacute MI patients (3.0 ± 0.4 vs. 2.1 ± 0.3, $p < 0.0001$). Mean peri-infarct STIR ratio was also elevated early post-acute MI, compared with both subacute and chronic MI patients (2.5 ± 0.4 vs. 2.1 ± 0.2, and 2.5 ± 0.4 vs. 1.9 ± 0.2, respectively, all $p \leq 0.005$). In remote sectors, however, the STIR ratio was similar in the early post-acute, chronic MI, and control groups (2.1 ± 0.2 vs. 2.0 ± 0.3 vs. 1.9 ± 0.1, p = NS) and early post-acute and subacute MI patients (2.1 ± 0.2 vs. 2.0 ± 0.2, p = NS).

MIF and TGF-β1. The median [interquartile range] sampling times for MIF, TGF-β1, collagen markers, and NT-proBNP were 2.5 [1.7 to 4.5] days, 146.5 [99 to 181.5] days, and 2,366 [262 to 4,334] days for the post-acute, subacute, and chronic MI groups, respectively. MIF levels were significantly elevated in the early post-acute MI group compared with the subacute MI group (Fig. 3A). There was an inverse correlation between early post-acute MI MIF levels and mean global T1 time ($r = -0.6$, $p = 0.01$) (Fig. 3B). TGF-β1 levels were highest among early post-acute and chronic MI patients, but levels did not differ significantly between groups (Fig. 3C).

Serum collagen markers and NT-proBNP. No difference in PINP or PIIINP levels was observed across MI groups (Figs. 3D and 3E). However, Ln NT-proBNP was highest early post-acute MI (Fig. 3F). Global post-contrast myocardial T1 times correlated inversely with Ln NT-proBNP ($r = -0.5$, $p = 0.02$).

Table 3. LV Volume, Function, and Infarct Characteristics by CMR Between Early Post-Acute and Subacute MI Groups

	Early Post-Acute MI	Subacute MI	p Value
LV mass indexed, g/m^2	74.0 ± 13.8	65.4 ± 15.8	**0.001**
Delayed enhancement, g	28.6 ± 18.6	16.6 ± 8.0	**0.002**
Myocardial infarct size, %	19.2 ± 10.5	12.8 ± 5.6	**0.001**
LVEF, %	50.2 ± 7.3	52.8 ± 9.4	**0.01**
LVEDVi, ml/m^2	85.8 ± 16.5	90.3 ± 26.0	NS
LVESVi, ml/m^2	42.9 ± 12.7	43.9 ± 22.0	NS
Infarct ESWT, mm	8.4 ± 1.5	8.4 ± 1.9	NS
Infarct EDWT, mm	5.6 ± 1.2	5.2 ± 0.8	NS
Infarct ESWT, %	57.5 ± 31.9	65.0 ± 36.5	NS
Peri-infarct ESWT, mm	8.4 ± 1.4	8.1 ± 1.6	NS
Peri-infarct EDWT, mm	5.6 ± 0.8	5.0 ± 1.0	**0.03**
Peri-infarct ESWT, %	55.8 ± 23.0	70.8 ± 38.2	NS
Remote ESWT, mm	8.8 ± 1.3	8.3 ± 1.4	NS
Remote EDWT, mm	5.8 ± 1.1	5.3 ± 0.9	NS
Remote ESWT, %	59.6 ± 24.6	67.0 ± 27.9	NS
Infarct STIR	3.0 ± 0.4	2.1 ± 0.3	**<0.0001**
Peri-infarct STIR	2.5 ± 0.3	2.1 ± 0.2	**0.005**
Remote STIR	2.1 ± 0.2	2.0 ± 0.2	NS
Global STIR	2.4 ± 0.3	2.0 ± 0.2	**0.001**
Mean infarct T1 time	320 ± 69	349 ± 71	NS
Mean peri-infarct T1 time	395 ± 62	446 ± 74	**0.04**
Mean remote T1 time	434 ± 93	515 ± 68	**0.01**
Mean global T1 time	391 ± 75	464 ± 59	**0.002**

Values are mean ± SD. p values in **bold** are statistically significant.
STIR = short-tau inversion recovery; other abbreviations as in Tables 1 and 2.

DISCUSSION

This prospective study provides evidence of an acute remodeling response in the remote noninfarcted myocardium *early* following acute MI as evidenced by reduced systolic function in this region. The demonstration of shortened post-contrast myocardial T1 times in the remote myocardium is consistent with

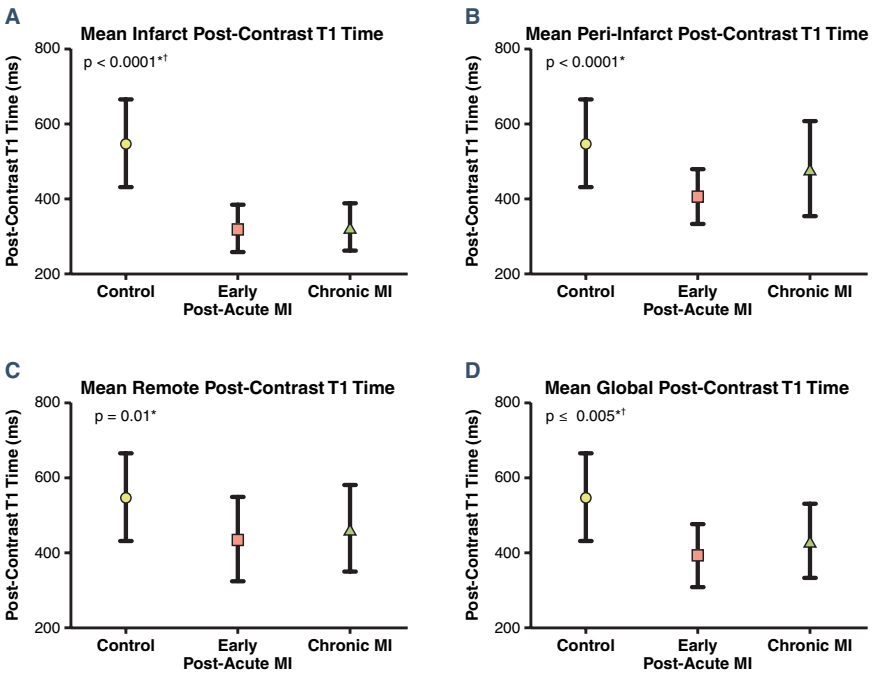

Figure 2. Post-Contrast T1 Times by Region

Data are presented as mean ± SD. **(A)** Mean infarct, **(B)** mean peri-infarct, **(C)** mean remote, and **(D)** mean global post-contrast T1 times for the control, early post-acute MI, and chronic MI groups. The mean global T1 time represents the mean T1 time of all infarct, peri-infarct, and remote sectors for a patient. *Control versus early post-acute MI; †control versus chronic MI. MI = myocardial infarction; NS = not significant.

ECM expansion due to interstitial changes suggestive of diffuse fibrosis, which is the histological hallmark of other more chronic forms of heart disease (4,13), with the absence of myocardial edema making a primary inflammatory or necrotic response in the noninfarcted myocardium less likely.

Such acute structural alterations in the remote myocardium may represent an additional mechanism to that of the traditional paradigm of LV remodeling post-MI due to the presence of an infarct scar and altered LV pressure and volume leading to progressive LV dilation and dysfunction (2). This complementary paradigm suggests that there are primary changes in the ECM that occur acutely in the noninfarct zone that also contribute to LV remodeling (3). In an experimental MI mouse model, Tsuda et al. (8) demonstrated that small infarcts without mechanical overload stimulated myocardial fibrosis development in the nonischemic myocardium distant from the infarct site as early as 72 h. However, the time course of acute changes and remodeling in the noninfarct zone in humans is not well understood, in part due to a prior lack of an in vivo imaging modality that could detect ECM expansion and quantify diffuse fibrosis.

Using CMR, we systematically characterized the evolution of LV remodeling and structural alterations in both infarcted and noninfarcted myocardium post-MI. Consistent with published data, we found an increase in indexed LV end-diastolic and end-systolic volumes with increasing chronicity of infarction (1,22). In the remote zones, we observed impaired regional systolic function as well as a profound shortening of post-contrast myocardial T1 times among early post-acute MI patients imaged within a week post-MI. In a subgroup analysis between early post-acute MI and control participants with similar age and sex, the remote post-contrast myocardial T1 times remained significantly shorter post-acute MI compared with controls. The prevalence of hypertensive status was also not different between controls and MI groups. Furthermore, we examined the possibility that the presence of acute interstitial edema may have also altered T1 times. However, we demonstrated that there was no difference in STIR ratio in the remote sectors of any MI groups compared with controls. A recent study utilizing T2 mapping also supports the absence of edema in the remote zone (23). Finally, variations in heart rate and renal function may affect myocardial T1 time (4); however, in this study, mean heart rate and renal function did not differ between control and MI groups.

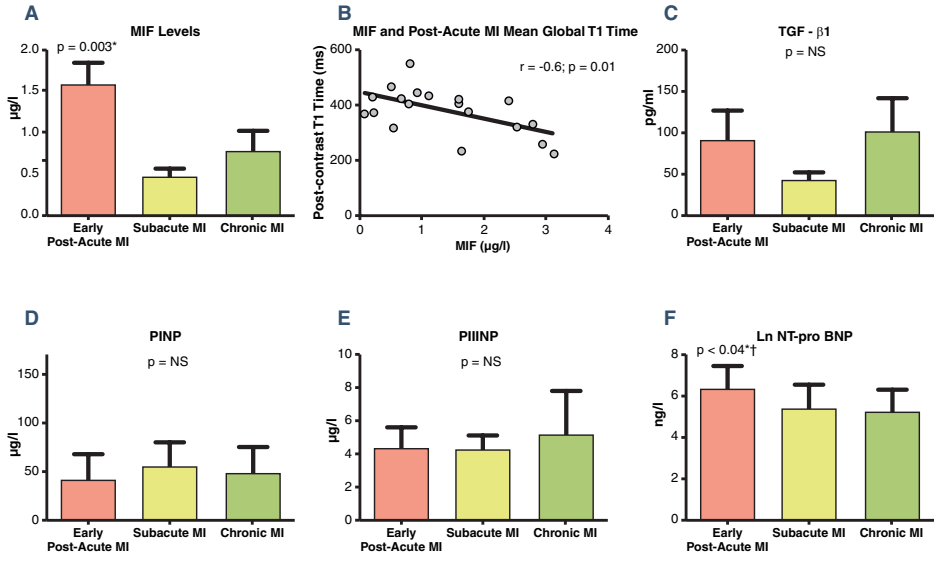

Figure 3. MIF, TGF-β1, Serum Collagen Markers, and NT-proBNP Levels

Data are presented as mean ± SD. **(A)** MIF levels of the control, early post-acute MI, and chronic MI groups. **(B)** MIF and post-acute MI mean global T1 time. **(C)** TGF-β1 levels, **(D)** PINP levels, **(E)** PIIINP levels, and **(F)** Ln NT-proBNP for the control, early post-acute MI, and chronic MI groups. *Early post-acute versus subacute MI; †early post-acute versus chronic MI. Ln NT-proBNP = logarithmic transformed N-terminal pro–B-type natriuretic peptide; MIF = macrophage migration inhibitory factor; PIIINP = N-terminal propeptide of type III procollagen; PINP = N-terminal propeptide of type I procollagen; TGF-β1 = transforming growth factor-β1; other abbreviations as in Figure 2.

Our data suggest that expansion of the ECM occurs early (within a week) in the noninfarct zone and persists into chronic stages. The exact nature of these early interstitial changes in the remote myocardium remains to be characterized. Prior animal studies support the presence of collagen in the non-infarct zone within the first few days after experimental MI (5,6,8). However, no studies in humans have characterized the evolution of structural alterations in both infarcted and noninfarcted myocardium and systolic dysfunction after MI. The observation of a partial recovery of remote T1 time in the subacute MI stage, but a strong trend toward shortening of remote T1 times in the chronic stage compared with controls suggests that early interstitial changes in the remote myocardium may partially regress and is consistent with data suggesting that interstitial fibrosis may be a reversible process (24), particularly with modulation of the renin-angiotensin-aldosterone axis (9,11,25) early post-MI.

The mechanisms that mediate the acute ECM changes throughout the noninfarct zone are ill defined and may involve myofibroblasts activated during the early inflammatory phase migrating out of the wound area, or neurohumoral factors (angiotensin II and TGF-β1) activating fibroblasts that are resident in the remote sites (26,27). For this reason, we sought to determine whether there was an association between the ECM changes identified by T1 mapping and putative mediators of myocardial inflammation and fibrosis. MIF is a pleiotropic cytokine that regulates a broad spectrum of acute and chronic inflammatory responses (28) and is thought to be released from preformed cytoplasmic myocyte stores early after MI (14,16). Myocardial MIF release may be one of the earliest secreted inflammatory mediators to be detected as a consequence of macrophage activation (16). MIF mediates ongoing inflammation by promoting production of other proinflammatory cytokines by macrophages (e.g., interleukin-1, TNF-α) (15) and is critical in the recruitment of macrophages and T cells into the infarcted myocardium (16), which then facilitates healing by scar formation. Our finding of an inverse correlation between serum MIF levels and mean global T1 time early post-acute MI suggests that there is biological coupling of the intense inflammatory response post-MI with development of ECM expansion and interstitial alterations in both the infarcted and noninfarcted myocardium. Similar to MIF, TGF-β1 levels, a well-known fibrogenic cytokine (17), trended higher in the acute than the subacute stages. However, we did not observe any correlations between regional post-contrast T1 times and TGF-β1 levels. This may be explained by the small study

sample size, the varied sampling time points post-acute MI, and that the systemic sampling of TGF-β1, in contrast to MIF sampling, may not detect a significant local or paracrine (myocardial) effect. Although we were not able to detect any significant differences in either PINP or PIIINP levels between the MI groups, Ln NT-proBNP was highest early post-acute MI and again correlated inversely with global post-contrast myocardial T1 times, suggesting that changes in the ECM are associated with a less compliant LV, which leads to higher NT-proBNP levels. It is possible that myocardial T1 mapping might be a more sensitive method for evaluation of ECM changes than systemic sampling of collagen markers because T1 mapping directly assesses myocardial tissue composition compared with systemic biomarkers, which are subject to many influences, including the timing post-MI and location of sampling. However, direct comparisons between T1 mapping and collagen markers have not yet been performed.

Study limitations. This was a small prospective study in highly selected groups of patients post-MI. Although we performed a subgroup analysis between early post-acute MI and controls of similar age and sex, and also found no differences in heart rate and renal function between MI groups and controls, there could be confounding effects from the heterogeneity within the MI groups with respect to MI location, medication use, and the success of recanalization in the chronic MI group that might impact MI size, rate of healing, and myocardial T1 times. Although age, sex, and diabetic and hypertensive status did not differ between MI groups and controls, it is possible that some confounding effect may be missed due to the small sample size. Similarly, the small sample size might have meant that the study was underpowered to detect a difference in collagen biomarkers. Additionally, some of the controls were also on antihypertensive therapy, which might have affected myocardial T1 time because of the antifibrotic properties of antihypertensive agents. We did not perform CMR within the first 2 days following infarction in the majority of the patients in the early post-acute MI group, and therefore, we are unable to provide data on the dynamic process of necrosis and infarct expansion within this early time frame. Another limitation of this study is the lack of histological data immediately after infarction to correlate ECM changes with noninfarct zone (remote) T1 time changes; however, several studies have now validated T1 mapping with histology (4,12,13). It is also possible that some selection bias was present in recruitment of chronic MI patients because many patients with LVEF <35% would have had cardioverter-defibrillator implantation and precluded CMR assessment. Finally, only 47% of chronic MI patients had angiographic assessment within 12 months of the study. However, the remainder all had recent nuclear myocardial perfusion stress testing to exclude ischemia.

CONCLUSIONS

This study suggests that physiological healing in acute MI is coupled with early remodeling and ECM expansion in the remote myocardium that persist into chronic stages, driven by the inflammatory response post-MI, mediated in part by MIF. The extent of ECM change correlates significantly with global and regional systolic dysfunction and has important prognostic implications because pharmacological modulation of the renin-angiotensin-aldosterone axis appears to limit ECM turnover in the remote myocardium during all stages of MI healing (10,29,30). Further prospective studies with larger sample sizes are needed to verify these important findings.

Reprint requests and correspondence: Dr. Andrew J. Taylor, Heart Centre, The Alfred Hospital, 3rd Floor, W.S. Philip Block, Commercial Road, Melbourne 3004, Victoria, Australia. *E-mail: a.taylor@alfred.org.au.*

REFERENCES

1. Beltrami CA, Finato N, Rocco M, et al. Structural basis of end-stage failure in ischemic cardiomyopathy in humans. Circulation 1994;89:151–63.
2. Pfeffer MA, Braunwald E. Ventricular remodeling after myocardial infarction. Experimental observations and clinical implications. Circulation 1990;81:1161–72.
3. Jugdutt BI. Ventricular remodeling after infarction and the extracellular collagen matrix: when is enough enough? Circulation 2003;108:1395–403.
4. Iles L, Pfluger H, Phrommintikul A, et al. Evaluation of diffuse myocardial fibrosis in heart failure with cardiac magnetic resonance contrast-enhanced T1 mapping. J Am Coll Cardiol 2008;52:1574–80.
5. Cleutjens JP, Verluyten MJ, Smiths JF, Daemen MJ. Collagen remodeling after myocardial infarction in the rat heart. Am J Pathol 1995;147:325–38.
6. Deten A, Holzl A, Leicht M, Barth W, Zimmer HG. Changes in extracellular matrix and in transforming growth factor beta isoforms after coronary artery ligation in rats. J Mol Cell Cardiol 2001;33:1191–207.

7. Delyani JA, Robinson EL, Rudolph AE. Effect of a selective aldosterone receptor antagonist in myocardial infarction. Am J Physiol Heart Circ Physiol 2001;281:H647–54.
8. Tsuda T, Gao E, Evangelisti L, Markova D, Ma X, Chu ML. Post-ischemic myocardial fibrosis occurs independent of hemodynamic changes. Cardiovasc Res 2003;59:926–33.
9. Zannad F, Alla F, Dousset B, Perez A, Pitt B, for the Rales Investigators. Limitation of excessive extracellular matrix turnover may contribute to survival benefit of spironolactone therapy in patients with congestive heart failure: insights from the randomized aldactone evaluation study (RALES). Circulation 2000;102:2700–6.
10. Pitt B, Remme W, Zannad F, et al. Eplerenone, a selective aldosterone blocker, in patients with left ventricular dysfunction after myocardial infarction. N Engl J Med 2003;348:1309–21.
11. Iraqi W, Rossignol P, Angioi M, et al. Extracellular cardiac matrix biomarkers in patients with acute myocardial infarction complicated by left ventricular dysfunction and heart failure: insights from the Eplerenone Post-Acute Myocardial Infarction Heart Failure Efficacy and Survival Study (EPHESUS) study. Circulation 2009;119:2471–9.
12. Scholz TD, Fleagle SR, Burns TL, Skorton DJ. Nuclear magnetic resonance relaxometry of the normal heart: relationship between collagen content and relaxation times of the four chambers. Magn Reson Imaging 1989;7:643–8.
13. Flett AS, Hayward MP, Ashworth MT, et al. Equilibrium contrast cardiovascular magnetic resonance for the measurement of diffuse myocardial fibrosis: preliminary validation in humans. Circulation 2010;122:138–44.
14. Yu CM, Lau CP, Lai KW, Huang XR, Chen WH, Lan HY. Elevation of plasma level of macrophage migration inhibitory factor in patients with acute myocardial infarction. Am J Cardiol 2001;88:774–7.
15. Calandra T, Bernhagen J, Mitchell RA, Bucala R. The macrophage is an important and previously unrecognized source of macrophage migration inhibitory factor. J Exp Med 1994;179:1895–902.
16. Yu CM, Lai KW, Chen YX, Huang XR, Lan HY. Expression of macrophage migration inhibitory factor in acute ischemic myocardial injury. J Histochem Cytochem 2003;51:625–31.
17. Desmouliere A, Geinoz A, Gabbiani F, Gabbiani G. Transforming growth factor-beta 1 induces alpha-smooth muscle actin expression in granulation tissue myofibroblasts and in quiescent and growing cultured fibroblasts. J Cell Biol 1993;122:103–11.
18. Ganame J, Messalli G, Dymarkowski S, et al. Impact of myocardial haemorrhage on left ventricular function and remodelling in patients with reperfused acute myocardial infarction. Eur Heart J 2009;30:1440–9.
19. Taylor AJ, Al-Saadi N, Abdel-Aty H, Schulz-Menger J, Messroghli DR, Friedrich MG. Detection of acutely impaired microvascular reperfusion after infarct angioplasty with magnetic resonance imaging. Circulation 2004;109:2080–5.
20. Abdel-Aty H, Boye P, Zagrosek A, et al. Diagnostic performance of cardiovascular magnetic resonance in patients with suspected acute myocarditis: comparison of different approaches. J Am Coll Cardiol 2005;45:1815–22.
21. Kim RJ, Wu E, Rafael A, et al. The use of contrast-enhanced magnetic resonance imaging to identify reversible myocardial dysfunction. N Engl J Med 2000;343:1445–53.
22. Hombach V, Grebe O, Merkle N, et al. Sequelae of acute myocardial infarction regarding cardiac structure and function and their prognostic significance as assessed by magnetic resonance imaging. Eur Heart J 2005;26:549–57.
23. Verhaert D, Thavendiranathan P, Giri S, et al. Direct T2 quantification of myocardial edema in acute ischemic injury. J Am Coll Cardiol Img 2011;4:269–78.
24. Krayenbuehl HP, Hess OM, Monrad ES, Schneider J, Mall G, Turina M. Left ventricular myocardial structure in aortic valve disease before, intermediate, and late after aortic valve replacement. Circulation 1989;79:744–55.
25. Brilla CG, Matsubara L, Weber KT. Advanced hypertensive heart disease in spontaneously hypertensive rats. Lisinopril-mediated regression of myocardial fibrosis. Hypertension 1996;28:269–75.
26. van den Borne SW, Diez J, Blankesteijn WM, Verjans J, Hofstra L, Narula J. Myocardial remodeling after infarction: the role of myofibroblasts. Nat Rev Cardiol 2010;7:30–7.
27. Shamhart PE, Meszaros JG. Non-fibrillar collagens: key mediators of post-infarction cardiac remodeling? J Mol Cell Cardiol 2010;48:530–7.
28. Bernhagen J, Calandra T, Bucala R. Regulation of the immune response by macrophage migration inhibitory factor: biological and structural features. J Mol Med 1998;76:151–61.
29. Kohno T, Anzai T, Naito K, et al. Angiotensin-receptor blockade reduces border zone myocardial monocyte chemoattractant protein-1 expression and macrophage infiltration in post-infarction ventricular remodeling. Circ J 2008;72:1685–92.
30. Pfeffer MA, Braunwald E, Moye LA, et al, for the SAVE Investigators. Effect of captopril on mortality and morbidity in patients with left ventricular dysfunction after myocardial infarction. Results of the survival and ventricular enlargement trial. N Engl J Med 1992;327:669–77.

Key Words: diffuse fibrosis ■ left ventricular remodeling ■ T1 mapping.